

## Accepted Manuscript

Title: Fe<sub>3</sub>O<sub>4</sub>@SiO<sub>2</sub>-imid-PMA<sup>n</sup> magnetic porous nanosphere as recyclable catalyst for the green synthesis of quinoxaline derivatives at room temperature and study of their antifungal activities

Author: Jaber Javidi Mohsen Esmailpour

PII: S0025-5408(15)30136-7  
DOI: <http://dx.doi.org/doi:10.1016/j.materresbull.2015.10.002>  
Reference: MRB 8424

To appear in: *MRB*

Received date: 20-4-2015  
Revised date: 1-9-2015  
Accepted date: 1-10-2015

Please cite this article as: Jaber Javidi, Mohsen Esmailpour, Fe<sub>3</sub>O<sub>4</sub>@SiO<sub>2</sub>-imid-PMA<sup>n</sup> magnetic porous nanosphere as recyclable catalyst for the green synthesis of quinoxaline derivatives at room temperature and study of their antifungal activities, Materials Research Bulletin <http://dx.doi.org/10.1016/j.materresbull.2015.10.002>

This is a PDF file of an unedited manuscript that has been accepted for publication. As a service to our customers we are providing this early version of the manuscript. The manuscript will undergo copyediting, typesetting, and review of the resulting proof before it is published in its final form. Please note that during the production process errors may be discovered which could affect the content, and all legal disclaimers that apply to the journal pertain.

**Fe<sub>3</sub>O<sub>4</sub>@SiO<sub>2</sub>-imid-PMA<sup>n</sup> magnetic porous nanosphere as recyclable catalyst for the green synthesis of quinoxaline derivatives at room temperature and study of their antifungal activities**

Jaber Javidi <sup>a,b\*</sup> jaberjavidi@sbmu.ac.ir, Mohsen Esmailpour<sup>c</sup>

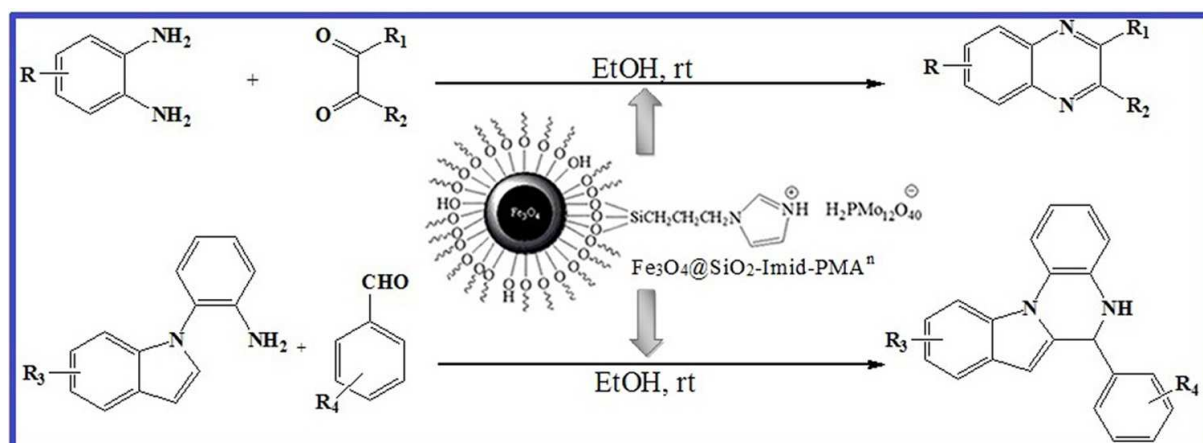
<sup>a</sup>Department of Pharmaceutics, School of Pharmacy, Shahid Beheshti University of Medical Sciences, Tehran, Iran

<sup>b</sup>Students Research Committee, School of Pharmacy, Shahid Beheshti University of Medical Sciences, Tehran, Iran

<sup>c</sup>Chemistry Department, College of Science, Shiraz University, Shiraz, Iran

\*Corresponding author. Tel.: +98 7116137738, fax: +98 7112286008.

## Graphical Abstract



**Highlights**

1. We developed simple and green procedure for the synthesis of quinoxaline derivatives.
2. BET and leaching of catalyst after each reaction cycle was investigated.
3. Antifungal activity of derivatives was investigated.

## Abstract

An efficient, simple, and green procedure for the synthesis of quinoxaline derivatives catalyzed by  $\text{Fe}_3\text{O}_4@\text{SiO}_2\text{-imid-PMA}^{\text{n}}$  nanoparticles at room temperature is described. This environmentally benign method provides several advantages such as mild reaction conditions, good to excellent yields, short reaction times, simple work-up and catalyst stability, easy preparation, heterogeneous nature and easy separation of the catalyst. Also, nanocatalyst can be easily recovered by a magnetic field and reused for the next reactions for at least 6 times without distinct deterioration in catalytic activity. SEM, BET, DLS and leaching of catalyst after each reaction cycle were investigated. Furthermore, antifungal activity of various derivatives against three phytopathogenic fungi (*A. alternata*, *P. oryzae*, and *A. brassicae*) was investigated.

**Keywords:** Quinoxalines; Green synthesis; Heterogeneous; Magnetic catalyst; Antifungal activity

## 1. Introduction

Quinoxalines are very important compounds due to their wide spectrum of biological activities behaving as anticancer [1], antiviral [2], antibacterial [3-5] and activity as kinase inhibitors [6]. Also, quinoxaline moieties have found applications in macrocyclic receptors [7], chemically controllable switches [8], building blocks in the synthesis of organic semiconductors [9], electroluminescent materials [10], organic semiconductors [11], dehydroannulenes [12], DNA cleaving agents [13], anti-inflammatory, anti-protozoal and anti-HIV [14,15]. The quinoxaline ring is also found in antibiotics such as echinomycin, leromycin and actinomycin [16-18].

Because of important applications of quinoxaline compounds in both medicinal and industrial fields, a number of protocols have been developed for the synthesis of quinoxaline derivatives. The condensation of amines with ketones has been used as a useful protocol for the synthesis of quinoxalines. For this transformation, several catalysts and reagents have been reported, including acetic acid [19], oxalic acid [20], sulfamic acid [21],  $H_6P_2W_{18}O_{62} \cdot 24H_2O$  [22],  $KHSO_4$  [23], Ni nanoparticles [24], iodine [25], gallium(III)triflate [26], montmorillonite K10 [27], polyanilinesulfate salt [28],  $ZrO_2/Ga_2O_3/MCM-41$  [29] and ionic liquids [17].

In addition, solid phase synthesis [30], microwave [31], bicatalyzed (bismuth and copper) oxidative coupling of peroxides and ene-1,2-diamines [32] were also reported. However, the critical product isolation procedure, long reaction time and harsh conditions of the above mentioned methods, non-recoverable catalysts, highly toxic and hazardous catalyst, limit their use in sustainable chemistry. Thus, the development of a new procedure for the synthesis of quinoxaline derivatives is still a desirable goal.

Nanoparticles (NPs) have been a topic of intense research mainly because of their unique physical and chemical properties compared with their bulk counterparts [33]. Metal oxide nanoparticles, with their potential applications in the fields of physics, chemistry, biology, and medicine have attracted increasing research attention from the past decades because of their interesting physical and chemical properties [34]. Magnetic nanoparticles have been widely used in the immobilization of enzymes [35], bio-separation [36], biosensor [37], immunoassay [38], targeted drug delivery and hyperthermia [39], environmental analysis [40] and catalysis [41-46].

In the field of catalysis, superparamagnetic nanoparticles have been utilized as catalyst supports for organic transformations such as alcohol hydrogenation [47], olefin hydrogenation [48], olefin hydroformylation [49], Sonogashira and Carbonylative Sonogashira reactions [50], Suzuki and Heck cross-coupling reactions [51], oxidation [52], dehalogenation [53], ring-opening polymerization of epsilon-caprolactone [54], asymmetric hydrogenation [55], as well as supports for biocatalysts [56,57] with high activity and selectivity. Recently, a number of functionalized Fe<sub>3</sub>O<sub>4</sub> nanoparticles have been employed in a range of organic transformations, and the studies on immobilization of metal and organo catalysts on silica coated iron oxide nanoparticles have been reported [58-61].

In recent years, heteropoly acids (HPAs) especially Keggin type have attracted increasing interest due to their high acidity, low toxicity and tunable redox properties [62]. Although HPAs are versatile compounds in their acidic form, their main disadvantages are high solubility in polar solvents and low surface area (<10 m<sup>2</sup>/g). Therefore, in a homogeneous reaction the isolation of the products and the reuse of the

catalyst after reaction become difficult [63]. Therefore, in order to overcome this problem, these materials disperse on supports (such as silica, acidic ion-exchange resins, active carbon and etc.) which possess large surface area. The use of support allows the heteropolyacids to be dispersed over a large surface area and increases their catalytic activity [64].

Therefore, as part of our researches to develop efficient and environmentally benign synthetic methods in organic chemistry [65], we report here an efficient, mild, green, and simple method for the preparation of quinoxalines from aryl/alkyl amines and different ketones using  $\text{Fe}_3\text{O}_4@\text{SiO}_2\text{-imid-PMA}^n$  as magnetic catalyst in EtOH.

## 2. Experimental

### 2.1. General methods

All chemicals were purchased from Merck or Fluka Chemical Companies. The progress of the reactions was followed by TLC using silica gel SILG/UV 254 plates and purification was achieved by silica gel column chromatography. Fourier transform infrared (FT-IR) spectra were recorded on a Shimadzu FT-IR 8300 spectrophotometer. The NMR spectra were recorded on a Bruker avance DMX 400MHz spectrometer in chloroform ( $\text{CDCl}_3$ ) using tetramethylsilane (TMS) as an internal reference. Scanning electron microscopy (SEM) image was obtained on Philips XL-30ESEM. Magnetic characterization was carried out on a vibrating sample magnetometer (Meghnatis Daghigh Kavir Co., Iran) at room temperature. Molybdenum contents in the functionalized sample before and after catalytic reactions were estimated by inductively coupled plasma-atomic emission spectroscopy (ICP-AES). Melting points were recorded on a Buchi B-545 apparatus in open capillary tubes. Elemental analysis

was done on a 2400 series Perkin-Elmer analyzer. Therefore, all of the products were characterized by FT-IR,  $^1\text{H}$  NMR and  $^{13}\text{C}$  NMR, and also by comparison with authentic samples.

## 2.2. General procedure

### 2.2.1. Preparation of $\text{Fe}_3\text{O}_4@\text{SiO}_2$ Core-Shell

The core-shell  $\text{Fe}_3\text{O}_4@\text{SiO}_2$  nanospheres were prepared by a modified Stober method in our previous work [65]. In a typical procedure, the mixture of  $\text{FeCl}_3\cdot 6\text{H}_2\text{O}$  (1.3 g, 4.8 mmol) in water (15 ml) was added to the solution of polyvinyl alcohol (PVA 15000), as a surfactant, and  $\text{FeCl}_2\cdot 4\text{H}_2\text{O}$  (0.9 g, 4.5 mmol) in water (15 ml), which was prepared by completely dissolving PVA in water followed by addition of  $\text{FeCl}_2\cdot 4\text{H}_2\text{O}$ . The resultant solution was left to be stirred for 30 min in  $80\text{ }^\circ\text{C}$ . Then, hexamethylen tetraamine (HMTA) (1.0 mol/l) was added drop by drop with vigorous stirring to produce a black solid product when the reaction media reaches pH 10. The resultant mixture was heated on water bath for 2 h at  $60\text{ }^\circ\text{C}$  and the black magnetite solid product was filtered and washed with ethanol three times and was then dried at  $80\text{ }^\circ\text{C}$  for 10h. Then  $\text{Fe}_3\text{O}_4$  nanoparticle (0.5 g, 2.1 mmol) was dispersed in the mixture of ethanol (50 mL), deionized water (5 mL) and tetraethoxysilane (TEOS) (0.20 mL), followed by the addition of 5.0mL of NaOH (10 wt%). This solution was stirred mechanically for 30 min at room temperature. Then the product,  $\text{Fe}_3\text{O}_4@\text{SiO}_2$ , was separated by an external magnet, and was washed with deionized water and ethanol three times and dried at  $80\text{ }^\circ\text{C}$  for 10 h.

### 2.2.2. Preparation of $\text{H}_3\text{PMo}_{12}\text{O}_{40}$ nanoparticles ( $\text{PMA}^n$ )

$\text{PMA}^n$  nanoparticles were prepared in our previous work [66]. In a typical procedure, 5 mmol of bulk  $\text{H}_3\text{PMo}_{12}\text{O}_{40}$  ( $\text{PMA}^b$ ) was dispersed in 50 mL n-Octane and the resulting dispersion was stirred vigorously for 30 min at room temperature to form a homogeneous dispersion. This dispersion was transferred into a Teflon-lined stainless autoclave filling 80 % of the total volume. The autoclave was sealed and maintained at 150 °C for 12 h. The autoclave was then cooled to room temperature. Finally, the resulted powder was filtered and washed for several times by Octane, and dried in a vacuum at 80 °C for 12 h.

### 2.2.3. Preparation of $\text{Fe}_3\text{O}_4@\text{SiO}_2$ -imid- $\text{PMA}^n$

$\text{Fe}_3\text{O}_4@\text{SiO}_2$  (1 g) was added to the solution of 3-chlorotriethoxypropylsilane (1 mmol, 0.241 g) and imidazole (1 mmol, 0.0680 g) in *p*-xylene (20 mL) and the resultant mixture was under reflux for 24 h under nitrogen atmosphere. After refluxing for about 24 h, the mixture was cooled to room temperature, filtered by an external magnet and the product was washed with xylene to remove no reacted species and dried at 70 °C for 6 h.  $\text{Fe}_3\text{O}_4@\text{SiO}_2$ -imid (1.0 g) was added to an acetonitrile solution of  $\text{PMA}^n$  (1.0 mmol) in 20 mL was taken in a round-bottom flask. The mixture was refluxed for 24h under nitrogen atmosphere. After 24 h, the mixture was filtered by an external magnet, washed with acetonitrile and dichloromethane, and dried at 70 °C for 6h. Also, the same method was used for the synthesis of  $\text{Fe}_3\text{O}_4@\text{SiO}_2$ -imid- $\text{PMA}^b$  ( $\text{PMA}^n = \text{nano } \text{H}_3\text{PMo}_{12}\text{O}_{40}$ ,  $\text{PMA}^b = \text{H}_3\text{PMo}_{12}\text{O}_{40}$ ) (Scheme1) [67].

#### 2.2.4. General procedure for the preparation of quinoxaline derivatives

To a stirred solution of amine (1 mmol) and carbonyl compounds (1 mmol) in EtOH (5 mL) were added  $\text{Fe}_3\text{O}_4@\text{SiO}_2\text{-imid-PMA}^n$  (0.03g, 0.5 mol%). The progress of the reaction was followed by thin-layer chromatography (TLC). After completion of the reaction, ethyl acetate was added to the solidified mixture and the insoluble catalyst was separated by magnetic field. The filtrate was dried and organic medium was removed with a rotary evaporator under reduced pressure. The crude products were crystallized from ethanol to afford pure products for analytical measurements.

#### 2.3. Biological assay

Several derivatives of quinoxaline (Entry 26 to 35 from Table 2) were investigated for their antifungal activities against three phytopathogenic fungi (*A. alternata*, *P. oryzae*, and *A. brassicae*).

Potato dextrose agar (PDA) medium was prepared in the flasks. Selected compounds were dissolved in acetone, and the concentration of these compounds was fixed at 60 mg/mL. The medium was then poured into sterilized Petri dishes. All types of fungi were incubated in PDA at 30 °C for five day to get new mycelium for the antifungal assays, and a mycelia disk of approximately 5 mm diameter cut from culture medium was picked up with a sterilized inoculation needle and inoculated in the center of the PDA Petri dishes. Acetone mixed with PDA The control sample was prepared by mixing Acetone mixed with PDA, without any compounds.

The growths of the fungal colonies were measured and the inhibitory effects of the compounds on these fungi in vitro were calculated by the formula:

Percent of inhibition rate= $(C-T)\times 100/C$

where C represents the diameter of fungi for the control sample, and T represents the diameter of fungi on treated PDA. Results were shown in Fig. 1.

### 3. Results and discussion

In our previous work [67], the  $\text{Fe}_3\text{O}_4$ ,  $\text{Fe}_3\text{O}_4@\text{SiO}_2$  and  $\text{Fe}_3\text{O}_4@\text{SiO}_2\text{-imid-PMA}^n$  nano catalysts were characterized by various methods such as transmission electron microscopy (TEM), scanning electron microscopy (SEM), dynamic light scattering (DLS), Fourier transform infrared (FT-IR), vibrating sample magnetometer (VSM) and etc. As shown in Scheme.1  $\text{Fe}_3\text{O}_4@\text{SiO}_2\text{-imid-PMA}^n$  nanoparticles have spherical shapes with approximately 50 nm diameters. The size distribution of these is centered at a value of 55 nm. The magnetic properties of  $\text{Fe}_3\text{O}_4$ ,  $\text{Fe}_3\text{O}_4@\text{SiO}_2$ ,  $\text{Fe}_3\text{O}_4@\text{SiO}_2\text{-imid-PMA}^n$  nanoparticles were measured by VSM at room temperature. All the samples show a typical superparamagnetic behavior. The saturation magnetization of samples is 63.4, 39.7, 33.2 emu/g, respectively. Hysteresis phenomenon was not found and the magnetization and demagnetization curves were coincident.

XPS is an important method to distinguish  $\text{Fe}_3\text{O}_4$  and  $\text{Fe}_2\text{O}_3$  since their same crystalline structure but different valence state of iron ions. For the Fe 2p spectrum of  $\text{Fe}_3\text{O}_4@\text{SiO}_2\text{-imid-PMA}^n$  two peaks at 711 and 725 eV correspond to Fe 2p<sub>3/2</sub> and Fe 2p<sub>1/2</sub> of  $\text{Fe}_3\text{O}_4$ , respectively. Moreover, the absence of shakeup satellite peak situated at ~719 eV, which is the fingerprint of the electronic structure of  $\text{Fe}_2\text{O}_3$  also confirms the  $\text{Fe}_3\text{O}_4$  species rather than  $\text{Fe}_2\text{O}_3$ .

Mo ion has two valence state, +5 or +6 and show two distinct couple peaks at (231.4 and 234.3 eV) or (232.4 and 235.5 eV) respectively in the Mo 3d spectrum. In the Mo 3d XPS spectrum of  $\text{Fe}_3\text{O}_4@\text{SiO}_2\text{-imid-PMA}^n$  to peaks at 232.5 and 235.5 eV which correspond to Mo  $3d_{5/2}$  and  $3d_{3/2}$  respectively were observed. Therefore the Mo ion in  $\text{Fe}_3\text{O}_4@\text{SiO}_2\text{-imid-PMA}^n$  has +5 valence states.

Also, in this article, determination of molybdenum content was performed by inductively coupled plasma-atomic emission spectroscopy (ICP-AES). According to the ICP-AES analysis, the Mo content in the magnetic nanocatalyst was determined which revealed the presence of 218 and 196 ppm for  $\text{Fe}_3\text{O}_4@\text{SiO}_2\text{-imid-PMA}^n$  and  $\text{Fe}_3\text{O}_4@\text{SiO}_2\text{-imid-PMA}^b$  catalyst. The amounts of  $\text{PMA}^n$  and  $\text{PMA}^b$  immobilized on  $\text{Fe}_3\text{O}_4@\text{SiO}_2\text{-imid-PMA}^n$  and  $\text{Fe}_3\text{O}_4@\text{SiO}_2\text{-imid-PMA}^b$  were found to be 36.1 wt% (0.19 mmol/g) and 31.3 wt% (0.17 mmol), respectively.

In order to optimize this condensation reaction conditions such as, solvents, amount of the nanocatalyst and also to check the versatility of this method with substituted amines, the reaction was carried out under various conditions.

In a model condensation reaction, *o*-phenylenediamine (1 mmol) and benzil (1 mmol) were stirred at room temperature in the presence of catalytic amount of  $\text{Fe}_3\text{O}_4@\text{SiO}_2\text{-imid-PMA}^n$  (0.5 mol%) in ethanolic medium (Scheme2). The reaction was completed in 5 min.

In order to evaluate the optimum amount of catalyst required for this condensation, the reaction was carried out in the presence varying amount of the catalysts and the results are presented in Table 1. The best result was achieved by carrying out the reaction

with (0.5 mol%, 1 mmol, 1 mmol) ratio of  $\text{Fe}_3\text{O}_4@\text{SiO}_2\text{-imid-PMA}^n$  catalyst, *o*-phenylene diamine and benzil in EtOH (Table 1, entry1). The results show clearly that catalyst is effective for this transformation and in the absence of catalyst; the reaction did not take place even after higher reaction time (Table 1, entry 14). Use of a higher amount of catalysts did not improve the yield (Table 1, entries 13) while a decrease in the amount of catalysts decreases the yield (Table 1, entries 11, 12).

The effect of solvent was studied by carrying out the model reaction at different solvents (Table 1, entries 1-10). Among the solvents examined, ethanol was found to be the most effective solvent (Table 1, entry 1). Furthermore, the reaction also proceeded comparatively well in methanol, acetonitrile and ethyl acetate (Table 1, entries 2,4,6). For this reaction a protic solvent with high dielectric constant such as water and ethanol show better reaction yield, but organic substrate have less solubility in water than ethanol. Therefore the yield of reaction in water is less than ethanol and we selected ethanol as reaction medium.

The scope and generality of the present method was then further demonstrated by the condensation at room temperature of various ketones with amine derivatives using the optimized conditions and the results are presented in Table 2. The yields of products were highly dependent on the electronic demands of the substrate used. Results show that electron-donating groups at the phenyl ring of amine favored the formation of product (Table 2, entries 7-11, 28-32). In contrast, electron-withdrawing groups such as nitro, benzoyl and chloro, gave slightly lower yields (Table 2, entries 12-23). On the other hand, electron donating substituents associated with aromatic ketone

decreased the product yields (Table 2, entries 2,3,8,13,17,18,22,26,29-31,33) and the effect is contrary with electron withdrawing groups (Table 2, entry 4-6,9-11,14,15,19,20,23,27,32,34,35). Also, aliphatic 1,2-diamines afforded the corresponding quinoxaline derivatives in slightly lower yields and longer reaction times (Table 2, entries 24,25). Furthermore, it is to be noted that highly pure products were obtained using this simple procedure and in most cases no further purification was needed.

In order to show the merit of the present catalytic method for the synthesis of quinoxalines, we have compared our results obtained using  $\text{Fe}_3\text{O}_4@\text{SiO}_2\text{-imid-PMA}^n$ ,  $\text{Fe}_3\text{O}_4@\text{SiO}_2\text{-imid-PMA}^b$ , Nano  $\text{Fe}_3\text{O}_4$ ,  $\text{Fe}_3\text{O}_4@\text{SiO}_2$ ,  $\text{Fe}_3\text{O}_4@\text{SiO}_2\text{-imid}$ ,  $\text{PMA}^b$  and  $\text{PMA}^n$  with some of those reported in the literature. These data, which are shown in Table 3, revealed that  $\text{Fe}_3\text{O}_4@\text{SiO}_2\text{-imid-PMA}^n$  is a better catalyst than most of the conventional catalysts mentioned with respect to reaction times and yields of the obtained products.

$\text{Fe}_3\text{O}_4@\text{SiO}_2\text{-imid-PMA}^n$  magnetic catalyst can be easily separated by external magnetic field within several minutes without the need for a centrifugation or filtration step or a tedious workup of the final reaction mixture (Fig. 1). However, magnetic separation performance makes the nanoparticles more effective and convenient in applications.

Several derivatives of quinoxaline (Entry 26 to 30 from Table 2) were investigated for their antifungal activities against three phytopathogenic fungi (*A. alternata*, *P. oryzae*, and *A. brassicae*).

The antifungal activities of several derivatives of quinoxaline (Entry 26 to 35 from Table 2) were investigated against three phytopathogenic fungi (*A. alternata*, *P. oryzae*, and *A. brassicae*). As shown in Fig. 2, compounds 26, 29 and 33 exhibited the good and broad spectrum of antifungal activities against these fungi. Generally, when the hydroxy group was introduced at the 4-position on the E-ring, derivatives showed the potent activities. Moreover, addition of hydroxyl group at the 2-position on the E-ring of compound 28 gave compound 31, the antifungal activities of which were decreased as compared with compound 29 bearing hydroxyl group at the 4-position on the E-ring.

An important advantage of employing magnetic catalysts is that they can be easily recovered from the reaction media by means of an external magnetic field. The activity of the recycle catalysts were also examined under the optimized conditions. For this reason, the room temperature reaction of *o*-phenylenediamine and benzil was studied in EtOH in the presence of  $\text{Fe}_3\text{O}_4@\text{SiO}_2\text{-imid-PMA}^{\text{n}}$  and  $\text{Fe}_3\text{O}_4@\text{SiO}_2\text{-imid-PMA}^{\text{b}}$  catalysts. At the end of the reaction, the catalysts were recovered by external magnetic field, followed by ethyl acetate washing and dried at ambient temperature. The recycled catalysts were used for six reactions without observation of appreciable loss in its catalytic activity (Fig. 3).

To determine the degree of leaching of the PMA<sup>n</sup> species from the heterogeneous catalyst, the catalyst was removed by using a magnetic field and the molybdenum amount in reaction medium after each reaction cycle was measured through Inductively Coupled Plasma (ICP) analyzer. The analysis of the reaction mixture by the ICP technique showed that the leaching of H<sub>3</sub>PMo<sub>12</sub>O<sub>40</sub> was negligible (Fig.4a). SEM image of the catalyst after the six recycle have been represented in Fig. 4b. As shown in Fig. 4b, Fe<sub>3</sub>O<sub>4</sub>@SiO<sub>2</sub>-imid-PMA<sup>n</sup> nanoparticles had an average diameter of 80 nm. However, the SEM image illustrates that these particles are composed of some smaller particles, which this indicates that some of the Fe<sub>3</sub>O<sub>4</sub>@SiO<sub>2</sub>-imid-PMA<sup>n</sup> NPs agglomerate due to the magneto-dipole interactions between NPs.

Additionally, the size and surface area of catalysts after each reaction cycle was investigated by DLS and nitrogen physisorption method (BET) respectively and results are provided in Table 4. TEM image of Fe<sub>3</sub>O<sub>4</sub>@SiO<sub>2</sub>-imid-PMA<sub>n</sub> after sixth cycle was shown in Scheme 1. As shown, the size of catalysts will be increased after each cycle. Generally, leaching of nano H<sub>3</sub>PMo<sub>12</sub>O<sub>40</sub>, agglomeration and increasing of Fe<sub>3</sub>O<sub>4</sub>@SiO<sub>2</sub>-imid-PMA<sup>n</sup> size and decrease of surface area led to a decrease in the yield of reaction.

#### 4. Conclusion

In summary, the present study confirms the applicability of immobilization of phosphomolybdic acid nanoparticles on imidazole functionalized Fe<sub>3</sub>O<sub>4</sub>@SiO<sub>2</sub> as an effective and reusable catalyst for one-pot synthesis of quinoxaline derivatives. The

significant advantages of our protocol are: mild reaction conditions, short reaction times, excellent yields, nanocatalyst stability, simple work-up procedure and involvement of an efficient and recyclable catalyst. Also, antifungal activity of various derivatives against three phytopathogenic fungi was investigated and compounds 26, 29 and 33 exhibited the good antifungal activities against these fungi.

### Spectral Data

**6-(p-Hydroxyphenyl)-5,6-dihydro-indolo[1,2-a]quinoxaline (Table2, Entry 26).** Pale yellow solid, m.p. 147-149°C; <sup>1</sup>H NMR (400 MHz, CDCl<sub>3</sub>) δ: 4.11 (1H, s, NH), 4.92 (1H, s, OH), 5.42 (1H, s), 5.87 (1H, s), 6.80-6.88 (3H, m), 6.99-7.04 (2H, m), 7.11 (1H, t, J= 7.5 Hz), 7.22-7.28 (1H, m), 7.35 (2H, d, J= 8.7 Hz), 7.51 (1H, d, J= 7.5 Hz), 7.90-7.93 (1H, m), 7.98 (1H, d, J= 8.1 Hz); <sup>13</sup>C NMR (125 MHz, CDCl<sub>3</sub>) δ: 56.6, 100.1, 111.6, 115.5, 116.0, 116.9, 120.1, 120.8, 121.0, 122.5, 124.0, 127.3, 129.6, 129.8, 132.3, 134.2, 137.7, 139.6, 155.77; IR cm<sup>-1</sup>: 737, 746, 1230, 1454, 1509, 1598, 3309.

**6-(p-Nitrophenyl)-5,6-dihydro-indolo[1,2-a]quinoxaline (Table2, Entry 27).** Yellow solid, m.p. 168-169°C; <sup>1</sup>H NMR (400 MHz, CDCl<sub>3</sub>) δ: 4.22 (1H, s, NH), 5.63 (1H, s), 5.85 (1H, s), 6.90-6.91 (1H, m), 7.04-7.06 (2H, m), 7.15 (1H, t, J= 7.6 Hz), 7.27 (1H, t, J= 7.2 Hz), 7.52 (1H, d, J= 7.6 Hz), 7.65-7.67 (2H, m), 7.93-8.02 (2H, m), 8.23 (2H, d, J= 8.4 Hz); <sup>13</sup>C NMR (125 MHz, CDCl<sub>3</sub>) δ: 56.7, 100.8, 112.0, 116.5, 117.3, 121.0, 121.4, 121.5, 123.3, 124.3, 124.6, 127.5, 129.4, 129.7, 134.4, 136.9, 137.5, 147.6, 148.3; IR cm<sup>-1</sup>: 734, 747, 1353, 1455, 1511, 1598, 3330.

**6-Phenyl-5,6-dihydro-8-methylindolo[1,2-a]quinoxaline (Table2, Entry 28).** Pale yellow solid, m.p. 159-161°C; <sup>1</sup>H NMR (400 MHz, CDCl<sub>3</sub>) δ: 2.43 (3H, s, CH<sub>3</sub>), 4.16 (1H, s, NH),

5.51 (1H, s), 5.88 (1H, s), 6.84-6.86 (1H, m), 6.94 (1H, d, J= 7.2 Hz), 7.00-7.02 (2H, m), 7.15 (1H, t, J= 8.0 Hz), 7.41-7.45 (3H, m), 7.52-7.53 (2H, m), 7.84 (1H, d, J= 8.4 Hz), 7.92-7.94 (1H, m);  $^{13}\text{C}$  NMR (125 MHz,  $\text{CDCl}_3$ )  $\delta$ : 18.7, 57.3, 98.5, 109.3, 116.0, 116.9, 120.1, 121.2, 122.6, 123.9, 127.4, 128.4, 128.6, 128.8, 129.3, 130.4, 133.8, 137.6, 138.6, 140.1; IR  $\text{cm}^{-1}$ : 628, 700, 738, 768, 1282, 1435, 1505, 1557, 1598, 3335.

**6-(p-Hydroxyphenyl)-5,6-dihydro-8-methylindolo[1,2-a]quinoxaline (Table2, Entry 29).**

Pale yellow solid, m.p. 178-179°C;  $^1\text{H}$  NMR (400 MHz,  $\text{CDCl}_3$ )  $\delta$ : 2.44 (3H, s,  $\text{CH}_3$ ), 4.10 (1H, s, NH), 4.98 (1H, s, OH), 5.43 (1H, s), 5.88 (1H, s), 6.84 (3H, d, J= 8.8 Hz), 6.94-7.02 (3H, m), 7.15 (1H, t, J= 8.0 Hz), 7.37 (2H, d, J= 8.4 Hz), 7.83 (1H, d, J= 8.4 Hz), 7.90-7.93 (1H, m);  $^{13}\text{C}$  NMR (125 MHz,  $\text{CDCl}_3$ )  $\delta$ : 18.7, 56.7, 98.4, 109.3, 115.5, 115.9, 116.9, 120.1, 121.1, 122.5, 123.9, 127.4, 129.3, 129.8, 130.4, 132.4, 133.8, 137.7, 139.0, 155.7; IR  $\text{cm}^{-1}$ : 734, 766, 1221, 1276, 1427, 1508, 1568, 1597, 1610, 3308.

**6-(p-Methoxyphenyl)-5,6-dihydro-8-methylindolo[1,2-a]quinoxaline (Table2, Entry 30).**

Orange solid, m.p. 195-196°C;  $^1\text{H}$  NMR (400 MHz,  $\text{CDCl}_3$ )  $\delta$ : 2.44 (3H, s,  $\text{CH}_3$ ), 3.85 (3H, s,  $\text{OCH}_3$ ), 4.12 (1H, s, NH), 5.45 (1H, s), 5.87 (1H, s), 6.84-6.86 (1H, m), 6.94 (3H, d, J= 8.8 Hz), 7.00-7.02 (2H, m), 7.15 (1H, t, J= 8.0 Hz), 7.44 (2H, d, J= 8.4 Hz), 7.83 (1H, d, J= 8.0 Hz), 7.91-7.94 (1H, m);  $^{13}\text{C}$  NMR (125 MHz,  $\text{CDCl}_3$ )  $\delta$ : 18.7, 55.3, 56.7, 98.4, 109.3, 114.0, 115.9, 116.9, 120.0, 121.1, 122.5, 123.9, 127.4, 129.3, 129.6, 130.4, 132.2, 133.9, 137.8, 139.0, 159.8; IR  $\text{cm}^{-1}$ : 741, 764, 826, 1027, 1235, 1262, 1562, 1598, 3317, 3345.

**6-(o-Hydroxyphenyl)-5,6-dihydro-8-methylindolo[1,2-a] quinoxaline (Table2, Entry 31).**

White solid, m.p. 193-195°C;  $^1\text{H}$  NMR (400 MHz,  $\text{CDCl}_3$ )  $\delta$ : 2.42 (3H, s,  $\text{CH}_3$ ), 5.58 (1H, s), 5.93 (1H, s), 6.95-6.99 (4H, m), 7.05 (1H, t, J= 7.6 Hz), 7.13-7.21 (2H, m), 7.23-7.25 (1H,

m), 7.34-7.38 (1H, m), 7.81 (1H, d, J= 8.4 Hz), 7.94 (1H, d, J= 8.0 Hz);  $^{13}\text{C}$  NMR (125 MHz,  $\text{CDCl}_3$ )  $\delta$ : 18.7, 57.5, 99.3, 109.2, 117.1, 117.4, 117.8, 119.8, 121.5, 122.1, 122.4, 123.0, 123.9, 128.4, 129.3, 129.9, 130.4, 130.8, 134.2, 135.7, 136.0, 156.7; IR  $\text{cm}^{-1}$ : 731, 759, 824, 1245, 1278, 1490, 1510, 1561, 1592, 3298.

**6-(p-Nitrophenyl)-5,6-dihydro-8-methylindolo[1,2-a]quinoxaline (Table2, Entry 32).**

Yellow solid, m.p. 218-219°C;  $^1\text{H}$  NMR (400 MHz,  $\text{CDCl}_3$ )  $\delta$ : 2.44 (3H, s,  $\text{CH}_3$ ), 4.23 (1H, s, NH), 5.67 (1H, s), 5.86 (1H, s), 6.90-6.92 (1H, m), 6.97 (1H, d, J= 7.6 Hz), 7.04-7.08 (2H, m), 7.19 (1H, t, J= 7.6 Hz), 7.70 (2H, d, J= 8.4 Hz), 7.85 (1H, d, J= 8.8 Hz), 7.94-7.96 (1H, m), 8.27 (2H, d, J= 8.4 Hz);  $^{13}\text{C}$  NMR (125 MHz,  $\text{CDCl}_3$ )  $\delta$ : 18.7, 56.5, 98.9, 109.4, 116.2, 117.0, 120.7, 121.5, 123.1, 124.0, 124.2, 127.3, 129.1, 129.2, 130.6, 133.8, 136.6, 136.7, 147.4, 148.1; IR  $\text{cm}^{-1}$ : 730, 759, 1276, 1341, 1503, 1516, 1561, 1596, 3362.

**6-(p-Hydroxyphenyl)-5,6-dihydro-7-methylindolo[1,2-a]quinoxaline (Table2, Entry 33).**

Pale yellow solid, m.p. 205-206°C;  $^1\text{H}$  NMR (400 MHz,  $\text{CDCl}_3$ )  $\delta$ : 1.99 (3H, s,  $\text{CH}_3$ ), 5.59 (1H, s), 6.65 (2H, d, J= 8.0 Hz), 6.73-6.75 (1H, m), 6.93-6.95 (2H, m), 7.06 (2H, J= 8.4 Hz), 7.16-7.29 (2H, m), 7.54 (1H, d, J= 7.6 Hz), 7.86-7.89 (1H, m), 7.98 (1H, d, J= 8.8 Hz);  $^{13}\text{C}$  NMR (125 MHz,  $\text{CDCl}_3$ )  $\delta$ : 8.3, 54.6, 107.2, 111.7, 115.5, 116.2, 116.4, 118.9, 119.8, 120.3, 122.5, 123.6, 127.4, 128.7, 130.7, 132.9, 133.3, 134.1, 135.7, 155.2. IR  $\text{cm}^{-1}$ : 738, 752, 1172, 1220, 1453, 1507, 1596, 3302.

**6-(p-Nitrophenyl)-5,6-dihydro-7-methylindolo[1,2-a]quinoxaline (Table2, Entry 34).**

Yellow solid, m.p. 159-161°C;  $^1\text{H}$  NMR (400 MHz,  $\text{CDCl}_3$ )  $\delta$ : 2.12 (3H, s,  $\text{CH}_3$ ), 4.39 (1H, s, NH), 5.78 (1H, s), 6.76 (1H, d, J= 6.8 Hz), 6.94-7.01 (2H, m), 7.21-7.25 (1H, m), 7.30-7.36

(3H, m), 7.59 (1H, d, J= 8.0 Hz), 7.89 (1H, d, J= 6.8 Hz), 8.01 (1H, d, J= 8.0 Hz), 8.07-8.09 (2H, m);  $^{13}\text{C}$  NMR (125 MHz,  $\text{CDCl}_3$ )  $\delta$ : 8.4, 53.9, 107.9, 111.9, 116.50, 116.58, 119.2, 120.5, 120.7, 123.0, 124.0, 124.1, 127.3, 127.8, 130.4, 131.0, 133.5, 134.4, 147.4, 148.8; IR  $\text{cm}^{-1}$ : 707, 738, 1342, 1455, 1508, 1597, 3368.

**6-(Furan-2-yl)-5,6-dihydro-7-methylindolo[1,2-a]quinoxaline** (Table2, Entry 35). Pale yellow solid, m.p. 44-46°C;  $^1\text{H}$  NMR (300 MHz,  $\text{CDCl}_3$ )  $\delta$ : 2.25 (3H, s,  $\text{CH}_3$ ), 4.52 (1H, s, NH), 5.79-5.82 (2H, m), 6.15 (1H, s), 6.81-6.97 (3H, m), 7.21-7.30 (3H, m), 7.60 (1H, d, J= 7.5 Hz), 7.83-7.86 (1H, m), 7.97 (1H, d, J= 8.1 Hz);  $^{13}\text{C}$  NMR (125 MHz,  $\text{CDCl}_3$ )  $\delta$ : 8.0, 48.2, 107.2, 107.6, 110.3, 111.7, 116.4, 119.1, 120.2, 120.4, 122.6, 123.6, 127.3, 130.1, 130.3, 133.5, 135.2, 142.2, 153.8; IR  $\text{cm}^{-1}$ : 741, 750, 803, 1012, 1092, 1458, 1507, 1598, 2918, 3360.

## Acknowledgements

Authors are grateful to the council of Iran National Science Foundation and University of Shiraz for their unending effort to provide financial support to undertake this work.

## References

- [1] C.W. Lindsley, Z. Zhao, W.H.Leister, R.G. Robinson, S.F. Barnett, D. Defeo-Jones, R.E.Jones, G.D. Hartman, J.R. Huff, H.E. Huber, M.E. Duggan, *Bioorganic & Medicinal Chemistry Letters* (2005) 15 761-764.
- [2] M. Loriga, S. Piras, P. Sanna, G. Paglietti, *Farmaco*. 52 (1997) 157-166.
- [3] L.E. Seitz, W.J. Suling, R.C. Reynolds, *Journal of Medicinal Chemistry* 45 (2002) 5604-5606.
- [4] H. Y. Lü, S. H. Yang, J. Deng, Z. H. Zhang, *Australian Journal of Chemistry* 63 (2010) 1290-1296.
- [5] J. T. Hou, Y. H. Liu, Z. H. Zhang. *Journal of Heterocyclic Chemistry* 47 (2010) 703-706.
- [6] W. He, M.R. Myers, B. Hanney, *Bioorganic & Medicinal Chemistry Letters* 13 (2003) 3097-3100.
- [7] T. Mizuno, W. H. Wei, L. R. Eller, *Journal of the American Chemical Society* 124 (2002) 1134-1135.
- [8] M. J. Crossley, L. A. Johnston, *Chemical Communications* 10 (2002) 1122-1123.
- [9] S. Dailey, W. J. Feast, R. J. Peace, I. C. Sage, S. Till, E. L. Wood, *Journal of Materials Chemistry* 11 (2001) 2238-2243.
- [10] K. R. J. Thomas, M. Velusamy, J. T. Lin, C. H. Chuen, Y. T. Tao, *Chemistry of Materials* 17 (2005) 1860-1866.
- [11] D. Brien, M. S. Weaver, D. G. Lidzey, D. D. C. Bradley. *Applied Physics Letters* 69 (1996) 881-883.
- [12] O. Sascha, F. Rudiger, *Synlett* 9 (2004) 1509-1512.
- [13] L. S. Hegedus, M. G. Marc, J. W. Jory, P. B. Joseph, *The Journal of Organic Chemistry* 68 (2003) 4179-4188.
- [14] X. Hui, J. Desrivot, C. Bories, P.M. Loiseau, X. Franck, R. Hocquemiller, B. Fidadere, *Bioorganic & Medicinal Chemistry Letters* (2006) 16 815-820.

- [15] K. Yb, K. Yh, P. Jy, K. Sk, *Bioorganic & Medicinal Chemistry Letters* 14 (2004) 541-544.
- [16] Y.S. Beheshtiha, M.M. Heravi, M. Saeedi, N. Karimi, M. Zakeri, N.T. Hossieni, *Synthetic Communications* 40 (2010) 1216-1223.
- [17] D. Fang, K. Gong, Z. Fei, X. Zhou, Z. Liu, *Catalysis Communications* 9 (2008) 317-320.
- [18] T. M. Potewar, S. A. Ingale, K. V. Srinivasan, *Synthetic Communications* 38 (2008) 3601-3612.
- [19] Z. Zhao, D. D. Wisnoski, S. E. Wolkenberg, W. L. Leister. Y. Wang, C. W. Lindsley, *Tetrahedron Letter* 45 (2004) 4873-4876.
- [20] A. Hasaninejad, A. Zare, M.R. Mohammadizadeh, M. Shekouhy, *Arkivoc* 13 (2008) 28-35.
- [21] H.R. Darabi, S. Mohandessi, K. Aghapoor, F. Mohsenzadeh, *Catalysis Communications* 8 (2007) 389-392.
- [22] M.M. Heravi, K. Bakhtiari, F. F. Bamoharram, M. H. Tehrani, *Monatshefte für Chemie* 138 (2007) 465-467.
- [23] H. A. Oskooie, M. M. Heravi, K. Bakhtiari, S. Taheri, *Monatshefte für Chemie* 138 (2007) 875-877.
- [24] A. Kumar, S. Kumar, A. Saxena, A. De, S. Mozumdar, *Catalysis Communications* 9 (2008) 778-784.
- [25] S.V. More, M. N. V. Sastry, C. C. Wang, C. F. Yao, *Tetrahedron Letter* 46 (2005) 6345-6348.
- [26] J. J. Cai, J. P. Zou, X. Q. Pan, W. Zhang, *Tetrahedron Letter* 49 (2008) 7386-7390.
- [27] T. K. Huang, R. Wang, L. Shi, X. X. Lu, *Catalysis Communications* 9 (2008) 1143-1147.

- [28] C. Srinivas, C. N. S. S. P. Kumar, V. J. Rao, S. Palaniappan, *Journal of Molecular Catalysis A: Chemical* 265 (2007) 227-230.
- [29] S. Ajaikumar, A. Pandurangan, *Applied Catalysis A: General* 357 (2009) 184-192.
- [30] K. S. Sanjay, G. Priya, D. Srinivas, K. Bijoy, *Synlett* 14 (2003) 2147-2150.
- [31] G. Shymaprosad, K.A. Avijit, *Tetrahedron Letter* 43 (2002) 8371-8373.
- [32] S. Antoniotti, E. Donach, *Tetrahedron Letter* 43 (2002) 3971-3973.
- [33] M. Salavati-Niasari, J. Javidi, Mahnaz Dadkhah, *Combinatorial Chemistry & High Throughput Screening* 16 (2013) 458-462.
- [34] M. Salavati-Niasari, J. Javidi, *Journal of Cluster Science* 23 (2012):1019–1028.
- [35] Y. Yong, Y. Bai, Y. Li, L. Lin, Y. Cui, C. Xia, *Journal of Magnetism and Magnetic Materials* 320 (2008) 2350-2355.
- [36] J. Javidi, M. Esmaeilpour, M. Rajabnia Khansari, *RSC Advances* 5 (2015) 73268-73278.
- [37] T. T. Baby, S. Ramaprabhu, *Talanta* 80 (2010) 2016-2022.
- [38] L. Wang, X. Gan, *Microchimica Acta* 164 (2009) 231-237.
- [39] J. Jaber, E. Mohsen, *Colloids and Surfaces B: Biointerfaces* 102 (2013) 265-272.
- [40] Y. Li, X. Li, J. Chu, C. Dong, J. Qi, Y. Yuan, *Environmental Pollution* 158 (2010) 2317-2323.
- [41] M. Esmaeilpour, J. Javidi, F. Dehghani, F. Nowroozi Dodeji, *New Journal of Chemistry* 38 (2014) 5453-5461.
- [42] J. Deng, L. P. Mo, F. Y. Zhao, L. L. Hou, L. Yang, Z. H. Zhang, *Green Chemistry* 13 (2011) 2576-2584.
- [43] M. Esmaeilpour, J. Javidi, F. Nowroozi Dodeji, M. Mokhtari Abarghoui, *Journal of Molecular Catalysis A: Chemical* 393 (2014) 18-29.
- [44] B. L. Li, M. Zhang, H. C. Hu, X. Du, Z. H. Zhang, *New Journal of Chemistry* 38 (2014) 2435-2442.

- [45] M. Esmailpour, J. Javidi, F. Nowroozi Dodeji, M. Mokhtari Abarghousi, *Transition Metal Chemistry* 39 (2014) 797-809.
- [46] C. Yang, H. Zhao, Y. Hou, D. Ma, *Journal of the American Chemical Society* 134 (38) (2012) 15814–15821.
- [47] V. Polshettiwar, B. Baruwati, R. S. Varma, *Green Chemistry* 11 (2009) 127-131.
- [48] A. H. Lu, W. Schmidt, N. Matoussevitch, H. Bonnemann, B. Spliethoff, B. Tesche, E. Bill, W. Kiefer, F. Schuth, *Angewandte Chemie International Edition* 43 (2004) 4303-4306.
- [49] T. J. Yoon, W. Lee, Y. S. Oh, J. K. Lee, *New Journal of Chemistry* 27 (2003) 227-229.
- [50] M. Esmailpour, J. Javidi, M. Mokhtari Abarghousi, F. Nowroozi Dodeji, *Journal of the Iranian Chemical Society* 11 (2014) 499–510.
- [51] M. Esmailpour, J. Javidi, F. Nowroozi Dodeji, H. Hassannezhad, *Journal of the Iranian Chemical Society* 11 (2014) 1703–1715.
- [52] B. Dutta, S. Jana, A. Bhattacharjee, P. Gütllich, S.I. Iijima, S. Koner, *Inorganica Chimica Acta* 363 (2010) 696-704.
- [53] T. Hara, T. Kaneta, K. Mori, T. Mitsudome, T. Mizugaki, K. Ebitani, K. Kaneda, *Green Chemistry* 9 (2007) 1246-1251.
- [54] W. Long, C. S. Gill, S. Choi, C. W. Jones, *Dalton Transactions* 39 (2010) 1470-1472.
- [55] A. Hu, G. T. Yee, W. Lin, *Journal of the American Chemical Society* 127 (2005) 12486-12487.
- [56] K. S. Lee, M. H. Woo, H. S. Kim, E. Y. Lee, I. S. Lee, *Chemical Communications* (2009) 3780-3782.
- [57] C. G. C. M. Netto, L. H. Andrade, H. E. Toma, *Tetrahedron: Asymmetry* 20 (2009) 2299-2304.
- [58] V. Polshettiwar, R. Luque, A. Fihri, H. Zhu, M. Bouhrara, J.M. Basset. *Chemical Reviews* 111 (2011) 3036-3075.

- [59] S. Shylesh, V. Schunemann, W.R. Thiel, *Angewandte Chemie International Edition* 49 (2010) 3428-3459.
- [60] J. Govan, Y. K. Gun'ko, *Nanomaterials* 4 (2014) 222-241.
- [61] M. B. Gawande, P. S. Branco, R. S. Varma, *Chemical Society Reviews* 42 (2013) 3371-3393.
- [62] A. S. Dias, I. V. Kozhevnikov, *Journal of Molecular Catalysis A: Chemical* 305 (2009) 104-111.
- [63] L. T. Aany Sofia, A. Krishnan, M. Sankar, N. K. Kala Raj, P. Manikandan, P. R. Rajamohanan, T. G. Ajithkumar, *The Journal of Physical Chemistry C* 113 (2009) 21114-21122.
- [64] Z. Zhang, F. Zhang, Q. Zhu, W. Zhao, B. Ma, Y. Ding, *Journal of Colloid and Interface Science* 360 (2011) 189-194.
- [65] M. Esmailpour, A.R. Sardarian, J. Javidi, *Applied Catalysis A: General* 445-446 (2012) 359-367.
- [66] J. Javidi, M. Esmailpour, Z. Rahiminezhad, F. Nowroozi Dodeji, *Journal of Cluster Science* 25 (2014) 1511-1524.
- [67] M. Esmailpour, J. Javidi, M. Zandi, *Materials Research Bulletin* 55 (2014) 78-87.
- [68] B. Krishnakumar, R. Velmurugan, S. Jothivel, M. Swaminathan, *Catalysis Communications* 11 (2010) 997-1040.
- [69] Ch. Srinivas, Ch.N.S. Sai Pavan Kumar, V. Jayathirtha Rao, S. Palaniappan, *Catalysis Letters* 121 (2008) 291-296.
- [70] M.M. Heravi, K. Bakhtiari, M.H. Tehrani, N.M. Javadi, H.A. Oskooie, *Arkivoc* 16 (2006) 16-22.
- [71] M. M. Heravi, S. Taheri, K. Bakhtiari, H.A. Oskooie, *Catalysis Communications* 8 (2007) 211-214.

- [72] H. R. Darabi, K. Aghapoor, F. Mohsenzadeh, M. R. Jalali, S. Talebian, L. Ebadi-Nia, E. Khatemifar, A. Aghaee, *Bulletin of the Korean Chemical Society* 32 (2011) 213-218.
- [73] S. V. More, M. N. V. Sastry, C. F. Yao, *Green Chemistry* 8 (2006) 91-95.
- [74] H.R. Darabi, F. Tahoori, K. Aghapoor, F. Taala, F. Mohsenzadeh, *Journal of the Brazilian Chemical Society* 19 (2008) 1646-1652.
- [75] H. R. Darabi, K. Aghapoor, F. Mohsenzadeh, F. Taala, N. Asadollahnejad, A. Badiiei, *Catalysis Letters* 133 (2009) 84-89.
- [76] K. Niknam, D. Saberi, M. Mohagheghnejad, *Molecules* 14 (2009) 1915-1926.

## Figure Captions

**Fig. 1:** Photo images of magnetic field-responsive of  $\text{Fe}_3\text{O}_4@\text{SiO}_2\text{-imid-PMA}^n$  nanoparticles (before magnetic field (a) and under magnetic field (b)).

**Fig. 2.** Antifungal activities (inhibition %) of compounds 26-35 at 60 mg/mL.

**Fig. 3:** Recyclability of  $\text{Fe}_3\text{O}_4@\text{SiO}_2\text{-imid-PMA}^n$  and  $\text{Fe}_3\text{O}_4@\text{SiO}_2\text{-imid-PMA}^b$  in the condensation reaction of *o*-phenylenediamine with benzil at room temperature.<sup>a</sup>

<sup>(a)</sup> Reaction condition: benzil (1 mmol), *o*-phenylenediamine (1 mmol),  $\text{Fe}_3\text{O}_4@\text{SiO}_2\text{-imid-PMA}^n$  (0.5 mol%) or  $\text{Fe}_3\text{O}_4@\text{SiO}_2\text{-imid-PMA}^b$  (0.7 mol%) and EtOH (5 mL), room temperature.

**Fig.4:** (a)  $\text{PMA}^n$  leaching (%) in each reaction cycle; (b) SEM image of  $\text{Fe}_3\text{O}_4@\text{SiO}_2\text{-imid-PMA}^n$  nanoparticles after six reaction cycles.<sup>a</sup>

<sup>(a)</sup> Reaction condition: benzil (1 mmol), *o*-phenylenediamine (1 mmol),  $\text{Fe}_3\text{O}_4@\text{SiO}_2\text{-imid-PMA}^n$  (0.5 mol%) and EtOH (5 mL), room temperature.

**Scheme 1** Process for preparation of immobilization of  $\text{H}_3\text{PMo}_{12}\text{O}_{40}$  nanoparticles on imidazole functionalized  $\text{Fe}_3\text{O}_4@\text{SiO}_2$  nanoparticle.

**Scheme.2:** Preparation of quinoxaline derivatives catalyzed by  $\text{Fe}_3\text{O}_4@\text{SiO}_2\text{-imid-PMA}^n$ .

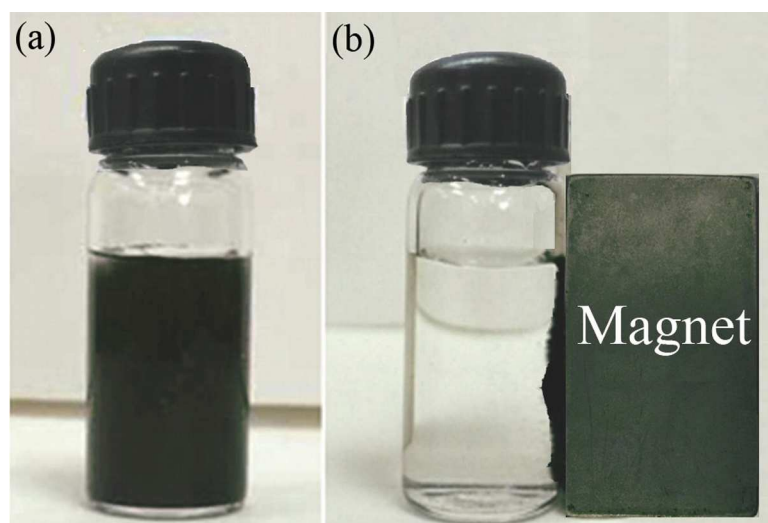


**Fig.1**

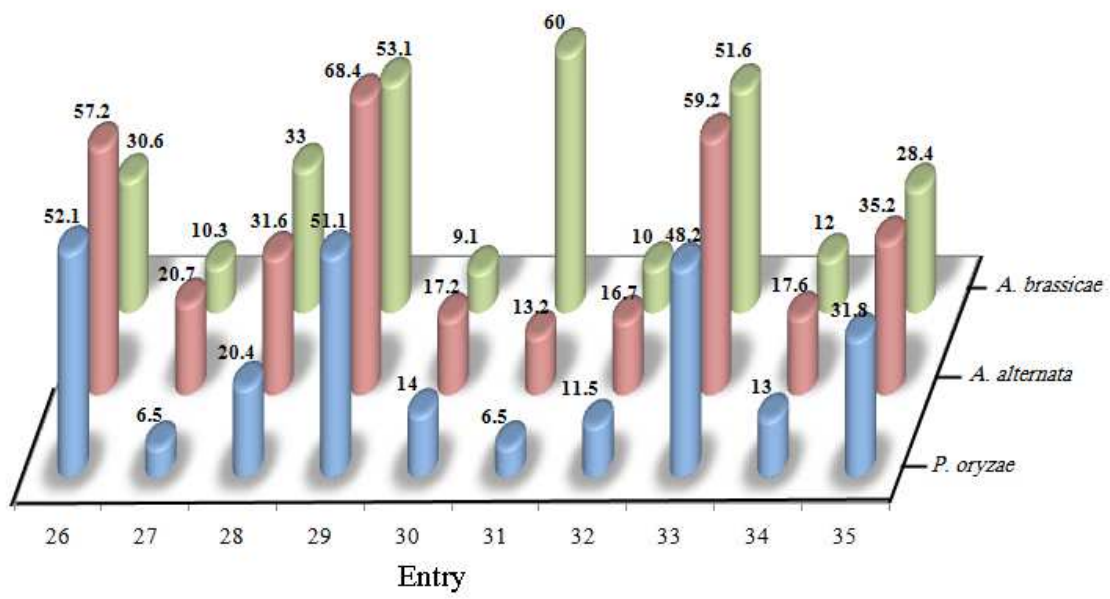
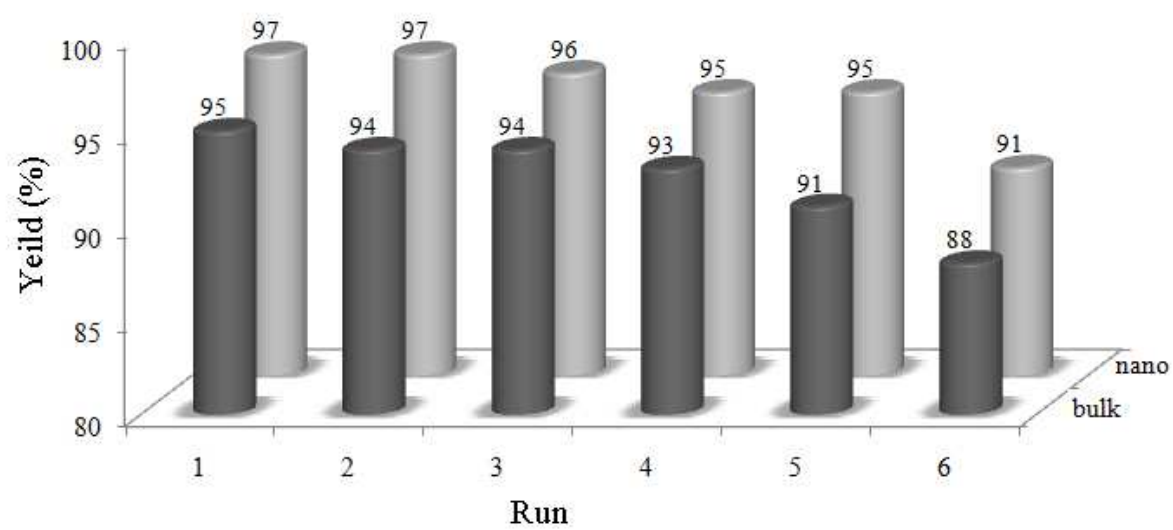


Fig. 2.



**Fig. 3.**

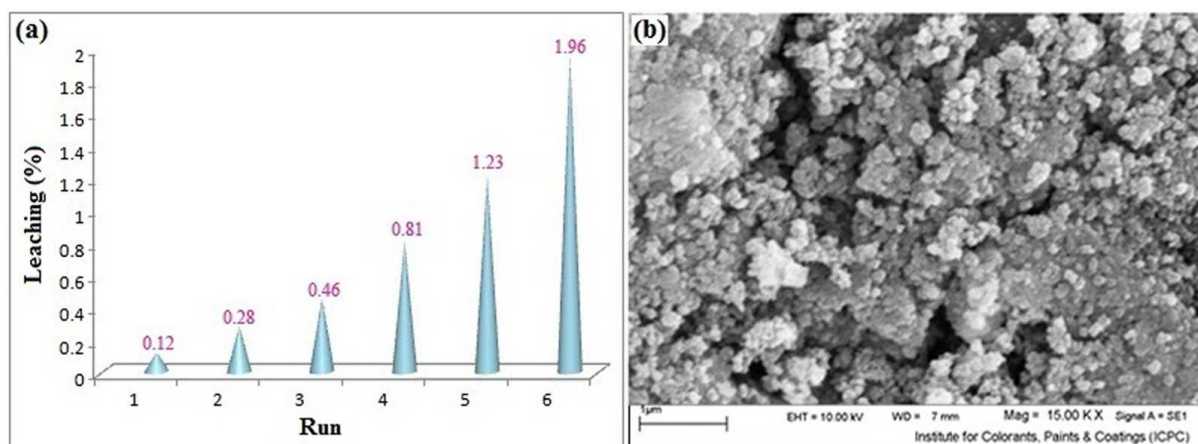
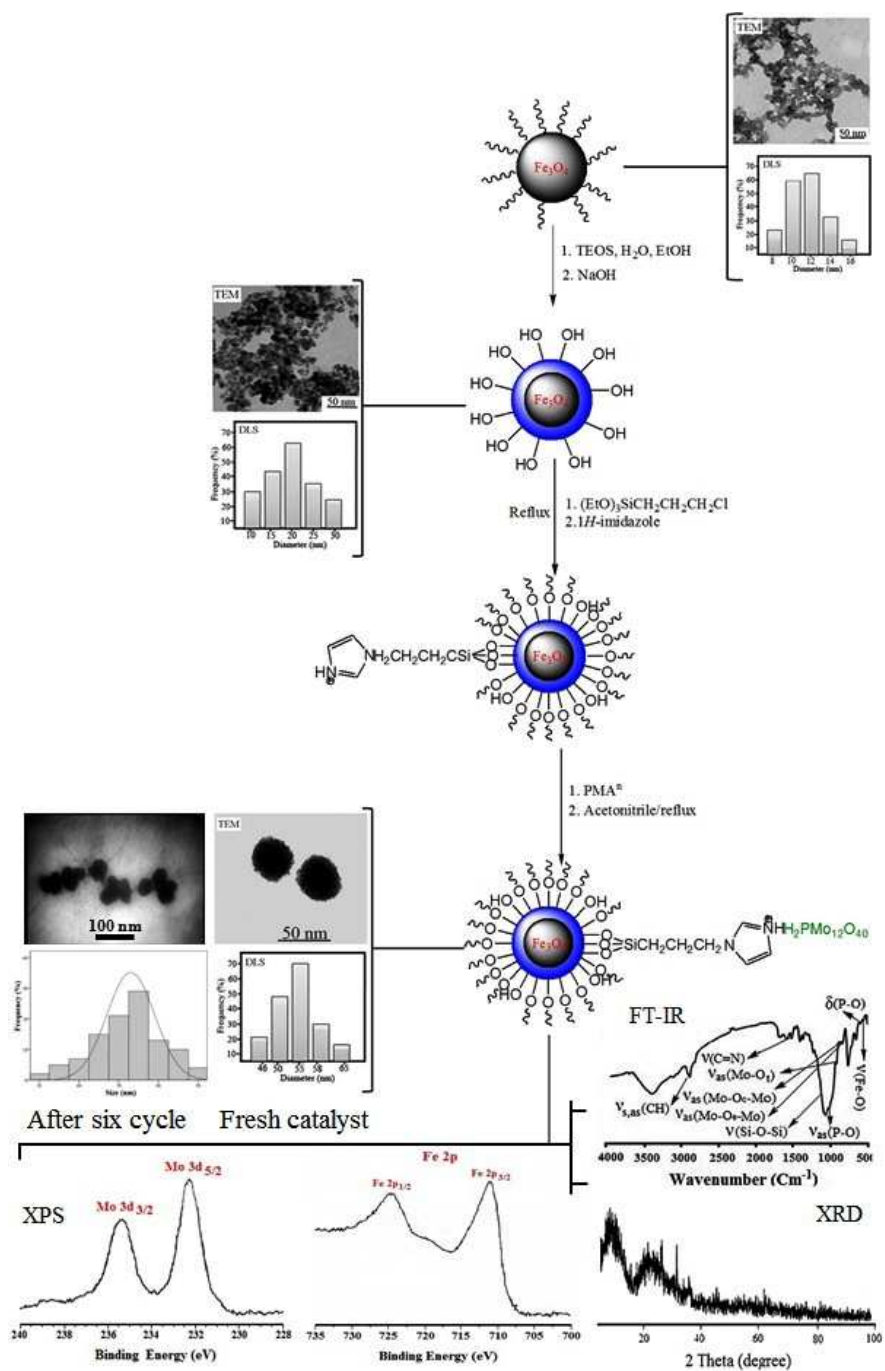
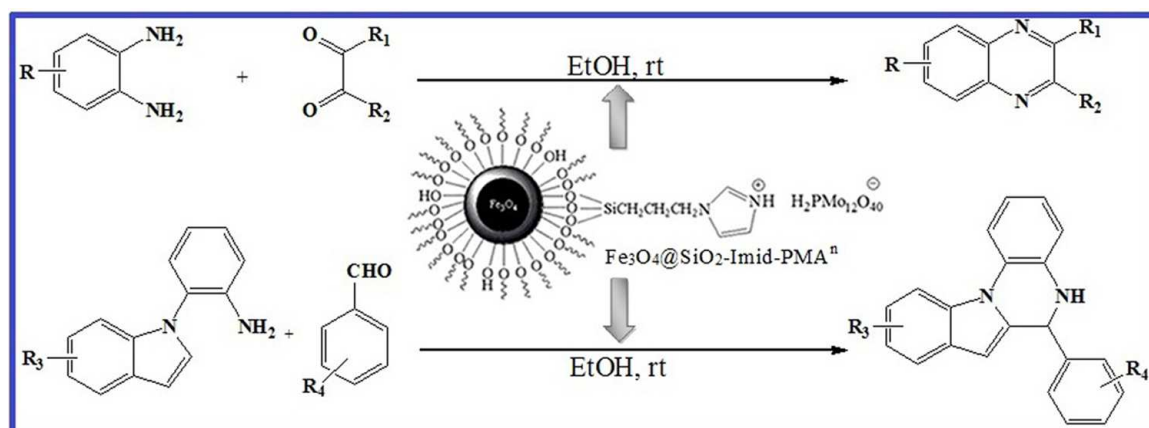


Fig.4.



Scheme 1



Scheme.2

## Tables

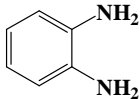
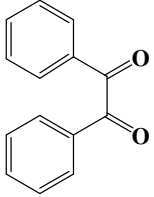
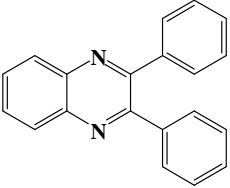
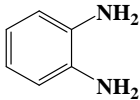
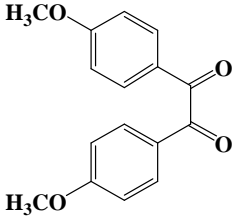
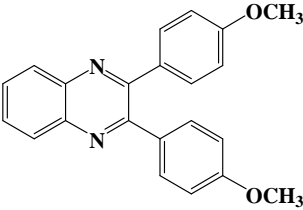
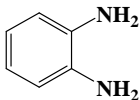
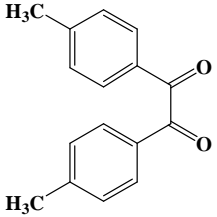
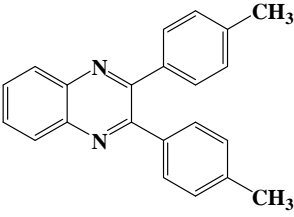
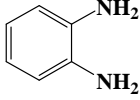
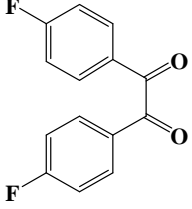
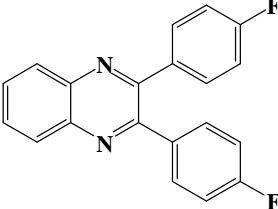
**Table.1:** Optimization of different proportions of Fe<sub>3</sub>O<sub>4</sub>@SiO<sub>2</sub>-imid-PMA<sup>n</sup> catalyst and also effect of solvent in the synthesis of 2,3-diphenylquinoxaline.<sup>a</sup>

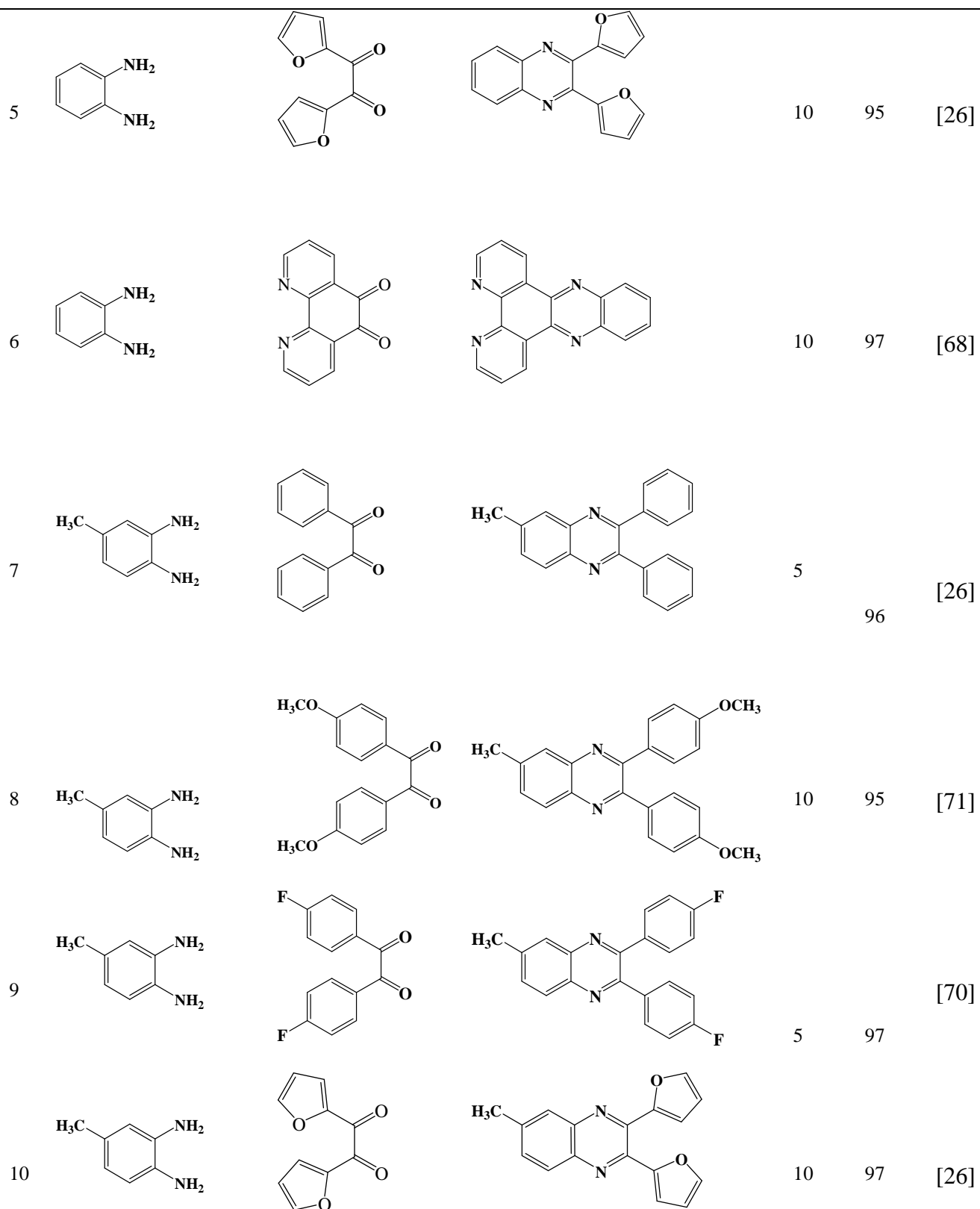
Entry	Solvent	The amount of catalyst (mol%)	Time (min)	Yield (%) <sup>b</sup>
1	EtOH	0.5	5	97
2	MeOH	0.5	5	92
3	H <sub>2</sub> O	0.5	30	23
4	CH <sub>3</sub> CN	0.5	15	84
5	DMF	0.5	15	76
6	CH <sub>3</sub> CO <sub>2</sub> Et	0.5	40	81
7	CHCl <sub>3</sub>	0.5	40	74
8	CH <sub>2</sub> Cl <sub>2</sub>	0.5	40	65
9	THF	0.5	60	17
10	Toluene	0.5	120	8
11	EtOH	0.2	60	23
12	EtOH	0.4	40	88
13	EtOH	0.6	5	96
14	EtOH	-	8h	8

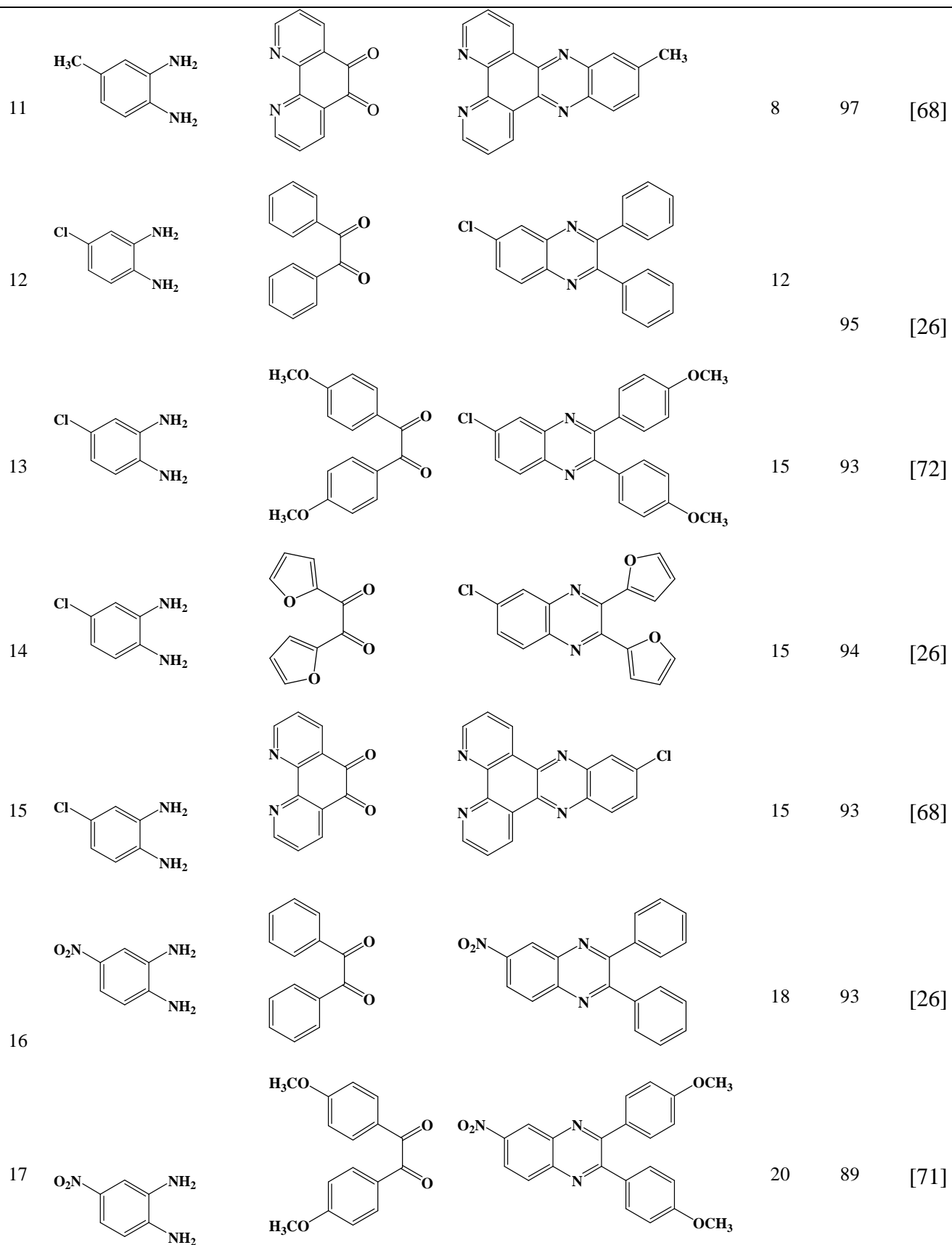
<sup>a</sup>Reaction condition: *o*-phenylenediamine (1mmol) and benzil (1mmol)

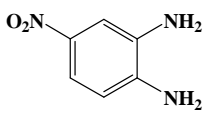
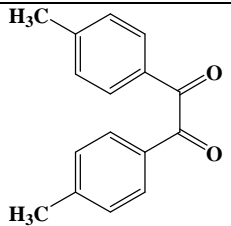
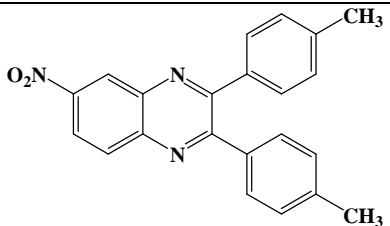
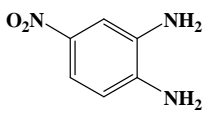
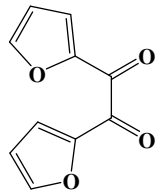
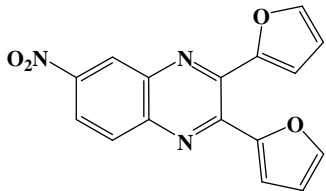
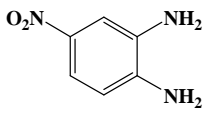
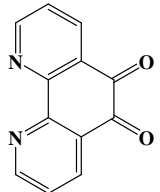
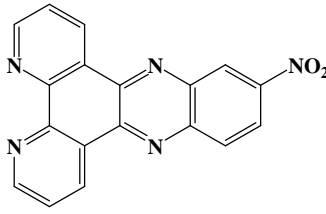
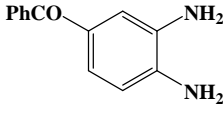
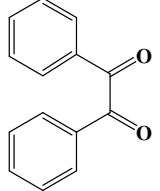
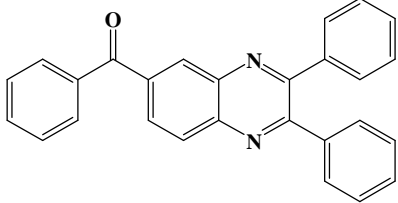
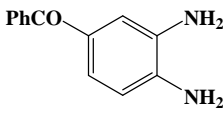
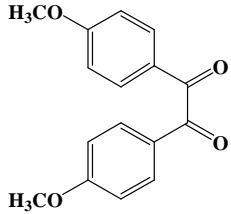
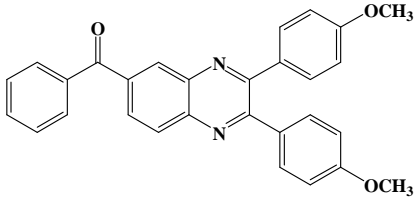
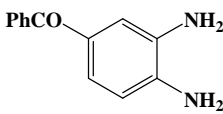
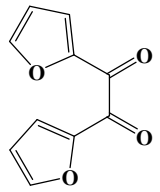
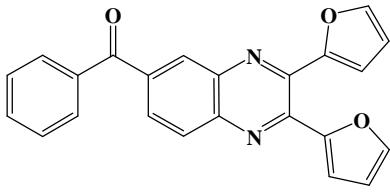
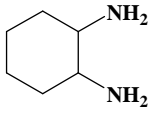
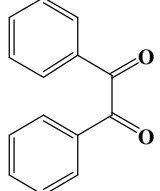
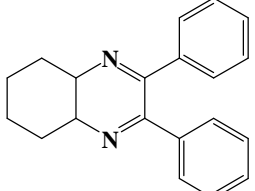
<sup>b</sup>Isolated yield.

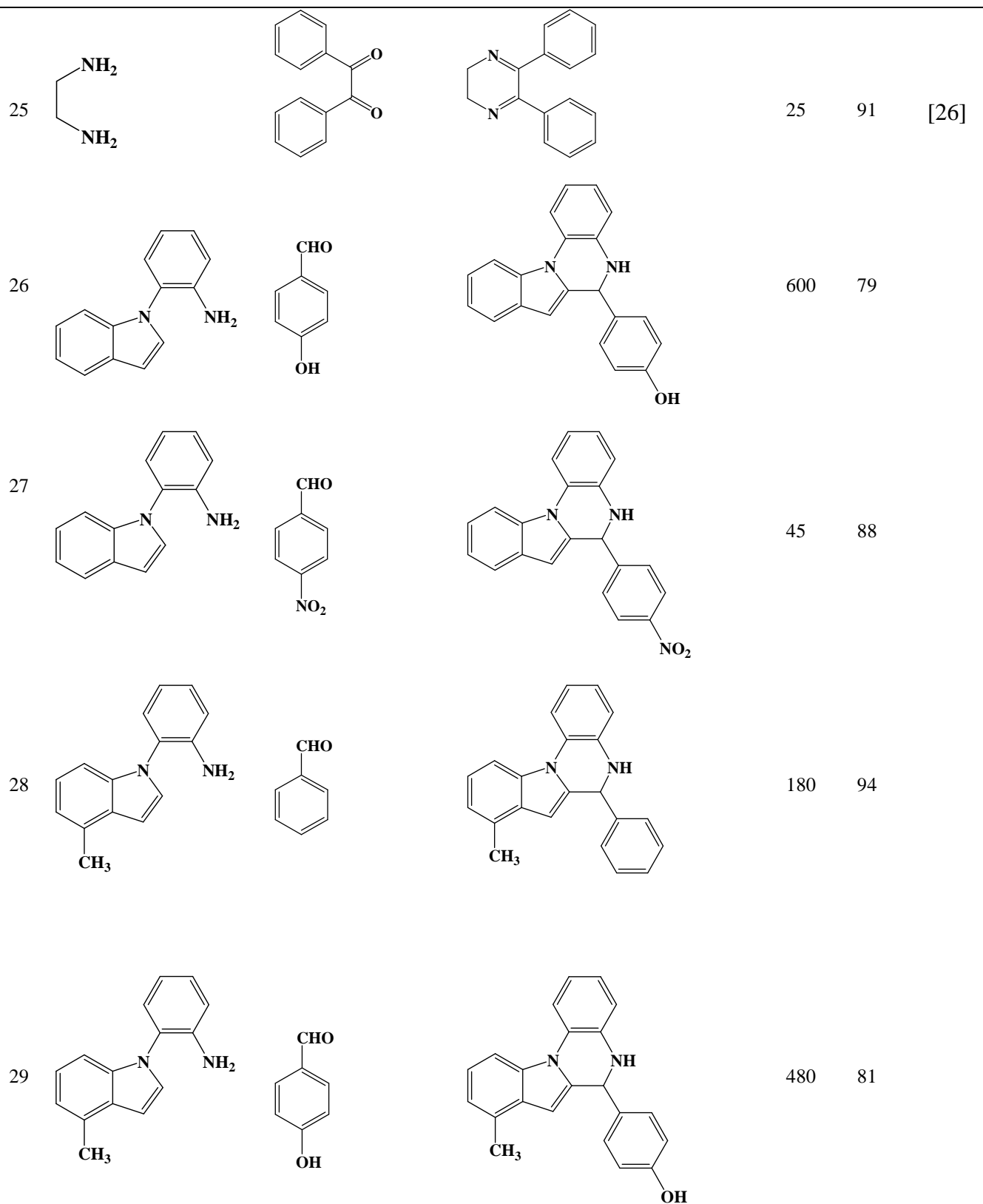
**Table.2:** Synthesis of quinoxaline derivatives catalyzed by  $\text{Fe}_3\text{O}_4@\text{SiO}_2\text{-imid-PMA}^n$  at room temperature.<sup>a</sup>

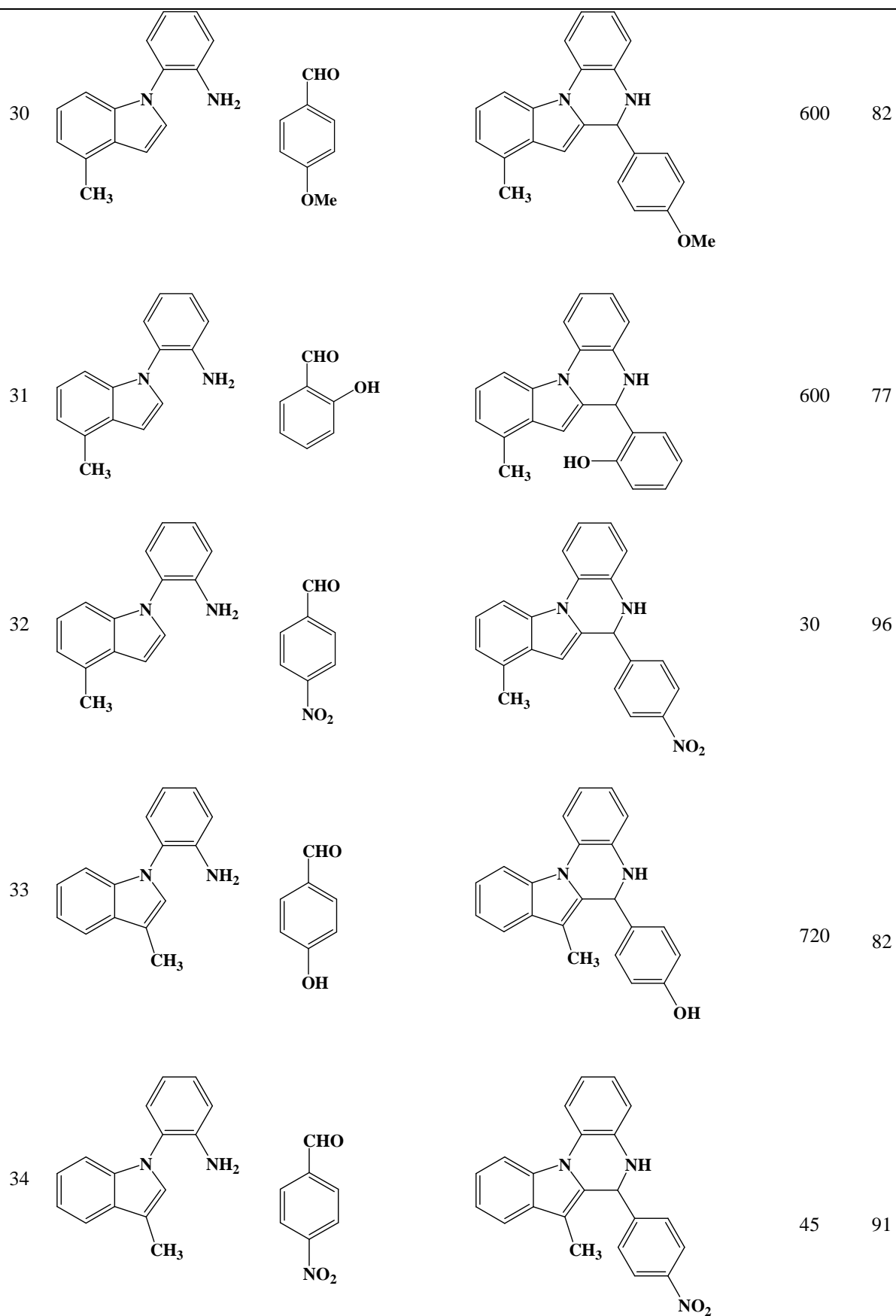
Entry	Diamine	Dicarbonyl	Product	Time (min)	Yield (%) <sup>b</sup>	[Ref]
1				10	97	[26]
2				15	94	[69]
3				10	94	[69]
4				7	97	[70]

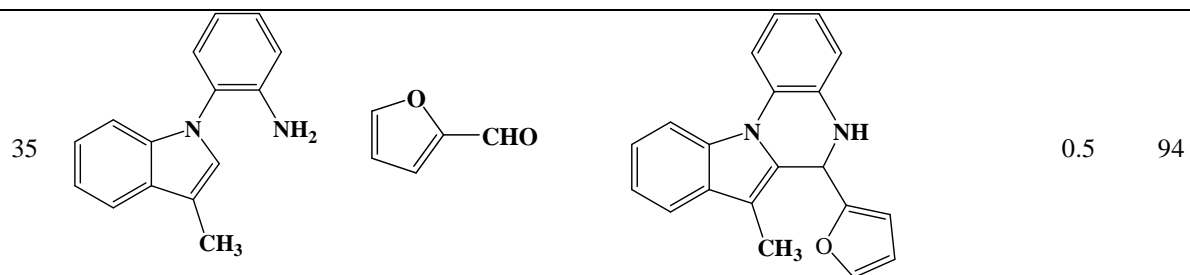




18				20	91	[69]
19				20	93	[26]
20				20	94	[68]
21				15	94	[26]
22				20	93	[69]
23				20	95	[26]
24				25	90	[73]



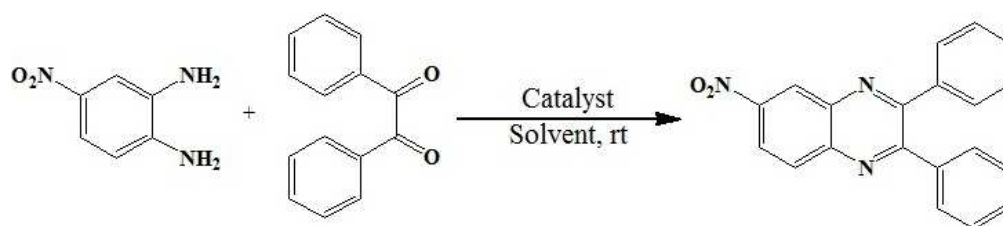




<sup>a</sup> Reaction condition: carbonyl compounds (1mmol), amine (1mmol),  $\text{Fe}_3\text{O}_4@\text{SiO}_2\text{-imid-PMA}^n$  (0.5 mol%), EtOH (5mL), room temperature.

<sup>b</sup> Isolated yield.

**Table.3:** Literature results for the synthesis of 6-nitro-2,3-diphenyl-quinoxaline at room temperature.



Entry	Catalyst	Solvent	Time	Isolated yield	[Ref]
			(min)	(%) <sup>a</sup>	
1	Fe <sub>3</sub> O <sub>4</sub> @SiO <sub>2</sub> -imid-PMA <sup>n</sup> (0.5 mol%)	C <sub>2</sub> H <sub>5</sub> OH	18	93	This work
2	Fe <sub>3</sub> O <sub>4</sub> @SiO <sub>2</sub> -imid-PMA <sup>b</sup> (0.7 mol%)	C <sub>2</sub> H <sub>5</sub> OH	35	90	This work
3	Nano Fe <sub>3</sub> O <sub>4</sub> (0.03g)	C <sub>2</sub> H <sub>5</sub> OH	120	81	This work
4	Fe <sub>3</sub> O <sub>4</sub> @SiO <sub>2</sub> (0.03g)	C <sub>2</sub> H <sub>5</sub> OH	120	76	This work
5	Fe <sub>3</sub> O <sub>4</sub> @SiO <sub>2</sub> -imid (0.03g)	C <sub>2</sub> H <sub>5</sub> OH	150	53	This work
6	PMA <sup>b</sup> (0.03 g)	C <sub>2</sub> H <sub>5</sub> OH	35	81	This work
7	PMA <sup>n</sup> (0.02 g)	C <sub>2</sub> H <sub>5</sub> OH	25	88	This work
8	Polyaniline–sulfate salt (5% w/w)	C <sub>2</sub> H <sub>4</sub> Cl <sub>2</sub>	40	90	[17]
9	Montmorillonite K10 (10% w/w)	H <sub>2</sub> O	600	70	[28]
10	17% ZrO <sub>2</sub> /4% Ga <sub>2</sub> O <sub>3</sub> /MCM-41	CH <sub>3</sub> CN	120	91	[29]
11	Sulfamic acid (80 mol %)	CH <sub>3</sub> OH	300	95	[74]
12	SbCl <sub>3</sub> /SiO <sub>2</sub> (2.5 mol %)	CH <sub>3</sub> OH	60	92	[75]
13	Gallium triflate (1 mol %)	C <sub>2</sub> H <sub>5</sub> OH	360	90	[26]
14	SBSSA (3.4 mol%)	EtOH/H <sub>2</sub> O [70/30(v/v)]	200	90	[76]
15	Ammonium chloride (200 mol %)	CH <sub>3</sub> OH	240	66	[74]
16	SnCl <sub>2</sub> /SiO <sub>2</sub> (5 mol %)	CH <sub>3</sub> OH	60	94	[72]

<sup>a</sup>Isolated yield.

**Table.4:** Mean particle size and specific surface area of Fe<sub>3</sub>O<sub>4</sub>@SiO<sub>2</sub>-imid-PMA<sup>n</sup> nanoparticles in each reaction cycle

<b>Run</b>	<b>Mean particle size (nm)<sup>a</sup></b>	<b>Specific surface area (m<sup>2</sup>/g)<sup>b</sup></b>
Fresh catalyst	55	422
1	57	416
2	59	402
3	63	397
4	66	384
5	71	366
6	74	341

<sup>a</sup>By DLS

<sup>b</sup>By BET